Human CardioChimeras: Creation of a Novel 'Next Generation' Cardiac Cell

Fareheh Firouzi [MS*1], Sarmistha Sinha Choudhury [MS*1], Kathleen Broughton [PhD1], Adriana Salazar [BS1], Mark A Sussman [PhD**1]

*co-first authors

[1] San Diego State University, Department of Biology and Integrated Regenerative Research Institute, San Diego, California.

Short title: **Human CardioChimera: Next Generation Cardiac Cell**

**Corresponding Author:

Mark A. Sussman, PhD

SDSU Heart Institute and Department of Biology

San Diego State University, 5500 Campanile Drive

San Diego, CA 92182

Phone: (619) 594-8632

Fax: (619) 594-8635

E-mail: heartman4ever@icloud.com

Subject codes: Basic Science Research; Cell Therapy; Myocardial Biology; Stem Cells; Cell Biology/Structural Biology

Abstract

Background: CardioChimeras (CCs) produced by fusion of murine c-kit$^+$ cardiac interstitial cells (cCIC) with mesenchymal stem cells (MSCs) promote superior structural and functional recovery in a mouse model of myocardial infarction (MI) compared to either precursor cell alone or in combination. Creation of human CardioChimeras (hCC) represents the next step in translational development of this novel cell type, but new challenges arise when working with cCICs isolated and expanded from human heart tissue samples. The objective of the study was to establish a reliable cell fusion protocol for consistent optimized creation of hCCs and characterize fundamental hCC properties.

Methods and Results: Cell fusion was induced by incubating human cCICs and MSCs at a 2:1 ratio with inactivated Sendai virus. Hybrid cells were sorted into 96-well microplates for clonal expansion to derive unique cloned hCCs, which were then characterized for various cellular and molecular properties. hCCs exhibited enhanced survival relative to the parent cells and promoted cardiomyocyte survival in response to serum deprivation in vitro.

Conclusions: The generation of hCC is demonstrated and validated in this study, representing the next step toward implementation of a novel cell product for therapeutic development. Feasibility of creating human hybrid cells prompts consideration of multiple possibilities to create novel chimeric cells derived from cells with desirable traits to promote healing in pathologically damaged myocardium.

Keywords: cell fusion; cardiac interstitial cells; mesenchymal stromal cells; cardiac; human

Clinical Perspective

- "Next generation" cell therapeutics will build upon initial findings that demonstrate enhanced reparative action of combining distinct cell types for treatment of cardiomyopathic injury.

- Differential biological properties of various cell types are challenging for optimization of delivery, engraftment, persistence, and synergistic action when used in combination.

- Creation of a novel hybrid cell called a CardioChimera overcomes limitations inherent to use of multiple cell types.

- CardioChimeras exhibit unique properties relative to either parental cell anticipated to be advantageous in cellular therapeutic applications.

- CardioChimeras have now been created and characterized using cells derived from human heart tissue, advancing initial proof of concept previously demonstrated with mice.

- CardioChimeras represent an engineered solution that can be implemented as a path forward for improving the outcome of myocardial cell therapy.

Non-standard Abbreviations and Acronyms

BDM   2,3-Butanedione 2-monoxime

CC   CardioChimera

cDNA   Complementary DNA

DAPI   4',6-diamidino-2-phenylindole

DMEM   Dulbecco's modified eagle medium

ES FBS   Embryonic stem cell FBS qualified

FACS   Fluorescence-Activated Cell Sorting

FBS   Fetal bovine serum

FGF2   Basic fibroblast growth factor

GAPDH   Glyceraldehyde 3-phosphate dehydrogenase

GATA4   GATA binding protein 4

GFP   Green fluorescent protein

HB-EGF   Heparin binding EGF like growth factor

HBSS   Hank's balanced salt solution

hCC   Human CardioChimera

hcCICs   Human **c-kit**+ cardiac interstitial cells (previous nomenclature of cardiac

          progenitor cells has been updated due to controversies in the field)

HEPES   4-(2-hydroxyethyl)-1-piperazineethanesulfonic acid

3

HGF	Hepatocyte growth factor
hMSC	Human mesenchymal stem cell
IL-6	Interlukin-6
I/R	Ischemia-reperfusion
LIF	Leukemia inhibitory factor
MI	Myocardial infarction
NRCM	Neonatal rat cardiomyocyte
PBS	Phosphate buffered saline
PECAM1	Platelet endothelial cell adhesion molecule or CD31
PI	Propidium iodide
SDF	Stromal derived factor
SMA	Smooth muscle actin
TNNT2	troponin T2, cardiac type

1 Introduction

2 Beneficial, albeit modest, effects of cell therapy for treatment of myocardial damage have been

3 established in extensive preclinical studies[1,2] as well as early clinical trial testing[3,4,5]. Improvement

4 of efficacy remains a primary focus of the cell therapy field with ongoing studies attempting to

5 define whether there is an optimal cell type or even a combination of cell types delivered

6 simultaneously to promote reparative remodeling[6,7]. The concept of creating an 'enhanced' cell

7 with augmented biological properties to promote healing remains a longstanding interest of our

8 group. Simply stated, we have sought to create 'unnatural solutions' to the natural limitations of

9 myocardial repair by ex vivo modification resulting in engineered cell products derived from c-

10 kit+ cardiac interstitial cells (cCICs) possessing enhanced survival, persistence, proliferation, and

11 many other desirable characteristics that deliver greater recovery from myocardial injury than

12 corresponding originating parental cells[8,9,10,11]. One example of this philosophy is the

13 CardioChimera, named for the fusion of cCICs and mesenchymal stem cells (MSCs) together into

14 a single hybrid cell that can be expanded in culture and used for adoptive transfer therapy to

15 mitigate myocardial infarction injury[8]. The seminal study of CardioChimeras was performed using

16 a homotypic murine model system with delivery murine CardioChimeras and results demonstrated

17 superiority of the CardioChimeras over either cCICs alone, MSCs alone, or the combination of

18 cCICs and MSCs delivered together as a single cell suspension. These promising findings

19 prompted subsequent studies to translate the murine findings into the human context but, working

20 with myocardial-derived human cells presents a new set of challenges to be overcome.

21 As opposed to murine cCICs and MSCs obtained from 2-3-month-old hearts with high yield

22 quantities[8], human cardiac cells are derived from small ventricular biopsy specimens[12]. Limited

23 source material results in lower yield of human myocardial-derived cells, and the relatively slow

1   proliferation of myocardial-derived human cells relative to mouse counterparts[12,13] further

2   hampers therapeutic manipulations. Furthermore, replicative senescence occurs much earlier in

3   culture passaging of human cells, whereas murine cardiac cells demonstrate significantly extended

4   passaging capability[8,14,15]. Another technical challenge posed by inherent species-specific biology

5   are differences between murine and human cells in response to experimental interventions[16].

6   Murine cells readily fuse and form polyploid hybrid cells[8] whereas human cells are much less

7   tolerant of polyploidy leading to genomic instability[17,18] that necessitates rigorous optimization of

8   culture conditions to overcome impaired expansion following fusion. Efficient and reproducible

9   creation of CardioChimeras is facilitated by use of murine cardiac cell populations from syngeneic

10   healthy young donors[8] unlike the individual patient-specific nature of human myocardial derived

11   cells with unavoidable sample characteristic variability[14]. Collectively, these challenges prompted

12   this study to demonstrate feasibility and reproducibility of human CardioChimera (hCC)

13   generation.

14   Concurrent isolation of three distinct CIC types comprised of cCIC, MSC, and endothelial

15   progenitor cells (EPC) from a single human myocardial tissue sample with optimized culture

16   condition was developed by our group[12]. Therefore, this protocol was employed to obtain human

17   cCIC and MSC for subsequent fusion proof of concept using low passage neonatal human

18   myocardial-derived cells. The rationale for using neonatal cells for feasibility testing is based upon

19   their more youthful biological phenotype of enhanced proliferation and survival, preservation of

20   telomere length, and decreased level of senescence relative to cells derived from heart failure

21   patients[14,15,19].

22   hCCs created in the present study represent novel hybrid cells with phenotypic properties

23   consistent with our previous observations of murine CCs. Having overcome the multiple

6

1   aforementioned challenges of human myocardial-derived cell utilization, cell fusion is a feasible

2   promising engineering approach to enhance functional properties of human cardiac cells and pave

3   the way for 'designer' hCC exhibiting enhanced reparative properties.

1   **Methods**

2   The authors declare that all supporting data are available within the article [and its online

3   supplementary files]. The data that support the findings of this study are available from the

4   corresponding author upon reasonable request.

5   **cCIC and MSC isolation**

6   The study was designed in accordance with and approved by the institutional review committees

7   at San Diego State University. Neonatal cells were derived from non-surgically obtained post-

8   mortem cardiac tissue. Cells were isolated as previously published[12]. Briefly, heart samples were

9   mechanically minced into $1mm^3$ pieces and digested in collagenase II (150 U mg/mL,

10 Worthington, LS004174) followed by brief low speed (850 rpm, for 2 minutes) centrifugation to

11 remove cardiomyocytes and tissue debris. The supernatant was subjected to magnetic activated

12 cell sorting (MACS) using c-kit conjugated microbeads (Miltenyi Biotec, #130-091-332) and c-

13 kit enriched cells were plated in human c-kit CIC media. The c-Kit negative population was further

14 purified by MACS for MSC surface markers CD90 and CD105. c-kit CICs and MSCs were

15 incubated at 37°C in 5% CO_2 and used for cellular fusion between passages 5 and 10. Media used

16 in the study are listed in Supplemental Table 1.

17 **Lentiviral constructs and stem cell infection**

18 Lentiviral plasmids and viral particles were created as previously described[8]. c-kit CICs and MSCs

19 were stably transduced at passage 6 with PGK-EGFP-Puro and PGK-mCherry-Bleo respectively

20 at a multiplicity of infection (MOI) of 40. Expression of EGFP and mCherry fluorescent proteins

21 in c-kit CICs and MSCs was confirmed by fluorescent microscopy as well as flow cytometry.

1   Lentivirally-modified cells were stabilized through multiple rounds of passaging and freeze/thaw

2   cycles before fusion experiments.

3   **Cell fusion and creation of hCCs**

4   Cell fusion was performed with GenomeONETM-CF EX Sendai Virus (Hemagglutinating Virus

5   of Japan-Envelope or HVJ-E) Envelope Cell Fusion Kit (Cosmo Bio, USA) using the suspension

6   method according to the manufacturer's protocol. Briefly, cCIC-EGFP and MSC-mCherry

7   populations were combined in 25µL of 1X cell fusion buffer at a ratio of 2:1 (total cell number of

8   100,000). The 2:1 ratio yielded the maximum number of double positive fused cells (hCCs) and

9   therefore was chosen for the study. Inactivated Sendai virus was added to the cell mixture and

10   incubated on ice for 5 minutes. Cell suspension was transferred to the 37°C incubator for 30

11   minutes with intermittent shaking every 5 minutes. Next, cells were plated in 2 ml fusion media

12   on a well of a 6-well dish. Media was changed after 24 hours and cells were then cultured in fusion

13   media for 4 days. Hybrid cells were identified and isolated by FACS sorting using parent cells in

14   pure as well as mixed (but not fused) as controls. hCCs were plated on a 96-well microplate (1 cell

15   per well) for clonal expansion. Clone nomenclature was based on well number in the plate. All

16   hCCs were used between passages 4 to 6 for experiments.

17   **Light microscopy and measurement of cell morphology**

18   Bright field images of hCCs and the parent cells were obtained using a LEICA DMIL microscope

19   and cell boundaries were outlined by image analysis using ImageJ software. Cell surface area and

20   length to width ratio were determined as previously described[20].

9

1   **Proliferation and doubling time**

2   c-kit CICs, MSCs and hCCs were plated on a 6-well dish at a density of 20,000 cells per well. At

3   three time points (days 1,3, and 5) cells were trypsinized and counted manually using a

4   hemocytometer. Cell proliferation rate was determined for each group as fold change over day 1.

5   Cell doubling times were calculated using online population doubling time software

6   (http://www.doubling-time.com/compute_more.php).

7   **Immunocytochemistry**

8   c-kit CICs, MSCs and hCCs were plated on a two-well chamber slide (15,000 per well). Staining

9   was performed following the protocol previously described[20]. Nuclei were stained with DAPI

10   diluted in 1X PBS at room temperature for 15 minutes. Cells were imaged using a Leica TCS SP8

11   confocal microscope. Antibodies and dilutions are listed in Supplemental Table 2.

12   **Immunoblot analysis**

13   c-kit CICs, MSCs and hCCs were plated on 100-mm plates. Protein cell lysates were collected

14   using 200 µl of SDS–PAGE protein sample buffer. Proteins were separated on a 4-12% NuPage

15   Novex Bis Tris gel (Invitrogen) and transferred onto a polyvinylidene fluoride (PVDF) membrane.

16   Non-specific binding sites were blocked using Odyssey blocking buffer (LI-COR) and proteins

17   were labeled with primary antibodies in 0.2% Tween in Odyssey blocking buffer overnight. After

18   washing, blots were incubated with secondary antibodies in 0.2% Tween 20 in Odyssey blocking

19   buffer for 1.5 hours at room temperature and scanned using the LICOR Odyssey CLx scanner.

20   Quantification was performed using ImageJ software. Antibodies and their dilutions are listed in

21   Supplemental Table 2.

22   **Real-Time PCR**

1   c-kit CICs, MSCs and hCCs were plated on 100-mm plates. RNA lysate was collected from the

2   culture and purified using Quick-RNA MiniPrep (Zymo Research). cDNA synthesis was

3   conducted using iScript cDNA Synthesis Kit (Bio Rad). qPCR was performed on a Bio-Rad CFX

4   real time cycler using iQ SYBR Green (Bio Rad) and gene specific primers. Signals were

5   normalized to 18S for analysis. Data were calculated using the $\Delta\Delta C(t)$ method. Primers are listed

6   in Supplemental Table 3.

7   **Ploidy and cytogenic analysis**

8   c-kit CICs, MSCs and hCCs were plated on a 6- well plate at a density of 50,000 cells per well.

9   Cells were collected the following day and centrifuged at 1200 rpm for 5 minutes, the pellet was

10   re-suspended in 70% ethanol, and stored at -20°C for at least 24 hours prior to use. After

11   centrifugation at 1300 rpm for 5 minutes, cell pellet was re-suspended in 300 ul of Propidium

12   Iodide incubated at 37°C for 15 minutes prior to flow cytometry analysis. Cytogenetic analysis of

13   c-kit CICs, MSCs, and hCCs (G4) plated at a density of 300,000 cells on 2500 mm^2 flasks was

14   performed by KaryoLogic, Inc (North Carolina; www.karyologic.com).

15   **Cell death assay**

16   For reactive oxygen injury, c-kit CICs, MSCs and hCCs were plated on a 6- well plate at a density

17   of 60,000 cells per well. Cells were subjected to low serum media for 24 hours (depleted to 25%

18   of growth media serum level) followed by 4 hours of hydrogen peroxide (350 µmol/L) treatment.

19   Annexin V and Sytox Blue staining was performed to label apoptotic and necrotic cells and cell

20   death was measured using FACS Aria (BD Biosciences).

21   For ischemia-reperfusion injury, cCICs, MSCs and hCCs were seeded on 6-well plates at a density

22   of 60,000 cells per well. The following day, media was replaced with Kreb's Heinsleit buffer (KH

23   buffer) to induce glucose starvation, and cells were transferred to a hypoxic incubator with 1%

1   oxygen tension for 3 hours to simulate ischemia. Cells were re-exposed to regular growth media

2   and incubated in a standard cell culture incubator with ambient (21%) oxygen for 24 hours to

3   simulate reperfusion. Annexin V and Sytox Blue staining was performed to label apoptotic and

4   necrotic cells and cell death was measured using FACS Aria (BD Biosciences). Cells cultured in

5   growth media in normoxic conditions and cells subjected to Kreb's Heinsleit buffer (KH buffer)

6   in hypoxic condition were used as the controls of the experiment to measure basal and hypoxia-

7   induced cell death, respectively. KH buffer and the respective media used inside the hypoxic glove

8   box were equilibrated in hypoxia overnight before starting the experiment.

9   **NRCM co-culture with stem cells**

10   NRCMs were isolated as previously described[21,22] and seeded in a 6-well dish at a density of

11   200,000 per well in M199 media with 15% fetal bovine serum (FBS). The following day, cells

12   were incubated in media with 10% FBS for 8 hours followed by 24-hour serum depletion in serum

13   free media. Stem cells (cCICs, MSCs, combination of cCICs and MSCs, hCCs) were added to the

14   culture at a 1:5 ratio. The slow growing clone B3 was excluded from this experiment due to a low

15   expansion rate. After 24 hours in co-culture, cells were stained with Annexin V and Sytox Blue.

16   Unlike CardioChimeras or their parent cells, the NRCMs were non-transduced allowing for

17   separation by fluorescent activated cell sorting (FACS) of negative cells (NRCMs) versus GFP+,

18   mCherry+ or GFP+/mcherry+ cells. Thus, parental and CardioChimera cells were removed from

19   the population for survival analysis of NRCMs, which was completed by flow cytometry using the

20   FACS Aria. Controls for the NRCMs included 1) culture in serum free media alone (SF), 2)

21   "rescue" by replenishment with M199 media + 10% serum, or 3) constant culture in M199 media

22   + 10% serum for the duration of the experiment.

23   **Statistical analysis**

1   All data are expressed as mean ±SEM. Statistical significance between two groups was assessed

2   using two-tailed t-test, or one-way ANOVA or two-way ANOVA for multiple comparisons, with

3   the Dunnett and Tukey tests as post hoc tests to compare groups to a control group in Graph Pad

4   Prism v5.0. or Microsoft excel. P<0.05 was considered statistically significant.

1   **Results**

2   **hCCs creation from c-kit CIC and MSC cell fusion**

3   Human c-kit CICs expressing GFP and human MSCs expressing mCherry, incubated in the

4   presence of inactivated RNA Sendai virus, underwent cellular fusion to form mononuclear hybrid

5   cells[23,24] (Figure 1A). A group of mixed c-kit CICs and MSCs without the viral treatment was

6   used as the negative control for the fusion experiment (Supplemental Figure 1E). Readily

7   detectable uniform fluorescence labeling of parental c-kit CICs and MSCs is required for optimal

8   yield of double fluorescent hybrids. Flow cytometry analysis shows 96.6% of c-kit CICs and 92%

9   of MSCs expressed EGFP and mCherry, respectively (Supplemental Figure 1A-D). Double

10   fluorescent hybrids were sorted into 96-well microplates for clonal expansion to derive hybrid

11   clones called hCCs. Five unique hCCs named D6, F1, G4, D2 and B3 were derived from five

12   independent fusion experiments with 1-4% efficiency (Table 1). Dual fluorescent positivity of

13   hCCs was validated by fluorescence microscopy (Supplemental Figure 2). Immunocytochemistry

14   with respective EGFP and mCherry antibodies confirmed integration of genomic content from

15   both parent cells into hCC that was maintained after clonal expansion and passaging in culture

16   (Figure 1B). Parent cells immunolabeled for EGFP and mCherry exhibited appropriate single

17   wavelength fluorescence signal, validating antibody specificity for their respective fluorophores

18   (Supplemental Figure 3). Immunoblotting results corroborate flow cytometry and microscopy

19   observations for expression of both fluorescent marker proteins (Figure 1C). Collectively, these

20   findings indicate successful cellular fusion and stability of the chimeric state after clonal

21   expansion.

22   **hCCs possess diploid DNA content**

1   Fusion of two parental lines resulted in elevated ploidy in murine CCs DNA content[8]. In

2   comparison, hCCs possess diploid (2n) DNA content comparable to the parent cells as assessed

3   using flow cytometry analysis (Figure 2A and Supplemental Figure 4). Since all hCCs exhibited

4   2n ploidy status, a representative line (hCC G4) was chosen for karyotypic analysis that confirmed

5   normal male karyotype with 46 chromosomes including XY as observed in G-banded spreads

6   (Figure 2B). Therefore, hCCs maintain normal 2n ploidy content relative to the parent cells, in

7   contrast to increased ploidy of murine CCs[8].

8   **hCCs phenotypic and proliferative characteristics resemble parent cells**

9   Murine CCs characteristics of survival and proliferation were comparable to parental lines albeit

10   with increased DNA content[8]. Cellular properties of select hCCs were assessed for phenotypic

11   traits of morphology and growth rate relative to parental lines, chosen to represent typical examples

12   for variability of hCC characteristics. Cellular morphology measured using bright field images of

13   the hCCs and parent cells reveals a range of cell surface area, length to width ratio (Figure 3).

14   hCCs D6, F1, and G4 exhibited cell surface area similar to cCICs that was significantly lower than

15   MSCs (Figure 3A). Length to width ratio of these clones was significantly greater compared to

16   MSCs and was comparable to that of cCICs (Figure 3B). Proliferation rate of these hCCs was

17   increased relative to parental cells with a doubling time of approximately 24 hours and were

18   therefore characterized as fast growth (Figure 3C,D). Cell surface area of hCC D2 was significantly

19   greater than the cCICs and similar to the MSCs (Figure 3A). Length to width ratio for hCC D2

20   was significantly decreased relative to cCICs, instead resembling that of MSCs (Figure 3B).

21   Proliferation rate of hCC D2 was intermediate compared to parent cells with a doubling time of 32

22   hours and was identified as a medium growth (Figure 3C,D). Lastly, hCC B3 cell surface area was

23   increased, length to width ratio was reduced, and proliferation rate was slow compared to either of

15

1 the parent cells, resulting in designation of slow growth (Figure 3A-D). Collectively, these data

2 profile phenotypic properties of hCCs with cell surface areas and length to width ratios that

3 correspond to their proliferative rates, consistent with previous findings for murine CCs[8].

4 **Profiling for commitment and secretory gene expression reveals hCC variability**

5 Gene expression profiling revealed significant heterogeneity between various murine CCs[8], so

6 commitment and secretory gene profiles for hCCs were assessed to find if similar diversity was

7 present. Cardiac lineage markers including cardiac type troponin T2 (TNNT2), GATA Binding

8 Protein 4 (GATA4), Platelet and Endothelial Cell Adhesion Molecule 1 (PECAM1), and smooth

9 muscle actin (SMA) were investigated by measuring mRNA expression level by qPCR analysis.

10 Early cardiac transcription factor GATA4 was significantly upregulated in all hCCs except B3 in

11 which GATA4 expression was not detected when compared to MSCs. When measured relative to

12 cCICs, GATA4 was approximately one-fold higher in F1, unchanged in D6 and G4, and

13 downregulated in D2 (Figure 4A). Cardiomyocyte marker TNNT2 level was reduced in fast

14 growing hCCs D6, F1 and G4 as opposed to medium and slow growing clones D2 and B3 (Figure

15 4B). PECAM1 level was higher in F1, G4 and D2 clones than in MSCs, but lower than cCICs.

16 PECAM1 was not detected in B3 (Figure 4C). All hCCs significantly downregulated SMA relative

17 to MSCs resembling closely to cCICs (Figure 4D). Collectively, these data demonstrate that fast-

18 growing hCCs upregulate expression of early cardiac transcription factor GATA4 and

19 downregulate expression of maturational cardiac marker TNNT2, reflective of their cardiac

20 progenitor-like phenotype. In contrast, medium and slow growing hCCs exhibit a more committed

21 mRNA profile from this cursory assessment with select transcripts.

22 hCCs were also analyzed for expression of pro-survival paracrine factors that mediate protective

23 effects. HB-EGF, a secreted glycoprotein involved in wound healing and cardiac development

16

1   [25,26], was significantly upregulated in hCC F1. In comparison, hCCs D6, G4 and D2 expressed

2   HB-EGF at levels intermediate between the two parent cell ranges. HB-EGF expression was

3   undetectable in hCC B3 clone (Figure 5A). HGF, a paracrine growth, motility and morphogenic

4   factor[27,28] was expressed at low levels in hCC D6, F1, G4 and D2, but at a comparable level to

5   MSCs in B3 (Figure 5B). hCCs F1 and D2 expressed high levels of chemotactic factor SDF relative

6   to cCICs but lower than in MSCs. SDF expression was downregulated in D6 and G4 and

7   undetectable in B3 (Figure 5C). FGF2, an important growth factor for wound healing, angiogenesis

8   and cellular proliferation[29] was highly upregulated in B3. hCC F1 and D2 increased FGF2

9   expression relative to cCICs and were more reminiscent of MSCs, while hCC D6 and G4 expressed

10   lower levels of FGF2 compared to both parent cells (Figure 5D). In summary, similar to what was

11   previously observed with murine CC[8], profiling of hCC reveals distinct transcriptome profiling

12   signatures between the clones.

13   **Survival in response to environmental stress is enhanced in hCC**

14   hCCs response to stress was assessed by serum deprivation with cell death quantitation by flow

15   cytometric measurement of necrosis and apoptosis. Cell death rates were similar between hCCs

16   and MSCs but lower than in cCICs (Figure 6A). Response to oxidative stress induced by hydrogen

17   peroxide treatment (350 µmol/L) in serum free conditions reveals significantly lower rates of

18   apoptosis and necrosis compared to either parental line with correspondingly higher rate of

19   survival (Figure 6B), consistently present even when media formulations for parental lines (cCIC

20   or MSC) are used for hCC culture (Supplemental Figure 5; D2 line). Simulated ischemia-

21   reperfusion injury was also used as an environmental stress with cells subjected to KH buffer in

22   hypoxia, and growth media in normoxia as experimental controls. Lower necrotic cell death was

23   found for all hCCs compared to parent cells. Similar apoptosis rates were observed comparing

1   hCCs to the parental lines with the exception of D2, which exhibited higher apoptotic cell death

2   (Figure 6C). Correspondingly, survival of all the hCCs except D2 was not significantly

3   different from either parental cell. Similar percentages of apoptotic, necrotic and live

4   cells were observed in experimental controls (Supplemental Figure 6). In conclusion,

5   unlike susceptibility to environmental stress in murine CCs similar to parent lines[8],

6   hCCs exhibit enhanced resistance to oxidative stress.

7   **Cardiomyocyte survival is enhanced by hCC co-culture**

8   Protective effects in response to serum deprivation challenge of NRCMs in vitro is similar between

9   murine CCs or their corresponding parental cells[8]. The protective effect of hCCs was similarly

10   assessed, with serum deprivation challenge of NRCMs that prompted significantly increased cell

11   death which was partially mitigated by addition of serum for 24 hours (Figure 7). Clone B3 was

12   excluded from further experiments due to slow expansion rate, undergoing replicative

13   senescence after passage 10 in culture. In comparison, lines D6, F1and G4 expansion

14   rate slowed after passage 10, yet had not reached replicative senescence. Line D2

15   maintained consistent proliferation rate for more than 10 passages, currently

16   expanded more than 27 passages without arrest (Supplemental Figure 7). NRCMs

17   showed improved survival mediated by each hCC in response to serum deprivation, co-culture

18   with hCC D2 yielding the highest rate of survival (Figure 7). NRCMs co-cultured with cCICs

19   exhibited high level of survival in response to serum deprivation. Co-culture of MSCs and hCCs

20   G4 partially rescued NRCMs resembling the effect of serum addition for 24 hours. hCCs D6 and

21   F1 exerted intermediate protective effect on NRCMs compared to parental cells while hCCs D2

22   provided the highest protective effect on NRCMs, exceeding even that of NRCMs in high serum.

23   Except for hCC G4 which exhibited protective effect similar to MSCs, most hCCs resembled

18

1   cCICs in co-culture effect upon NRCMs. Therefore, in contrast to murine CCs with protective

2   effect similar to their corresponding parent cells, hCCs exhibit individually distinct variability in

3   protective action.

1 **Discussion**

2 Myocardial repair and regeneration research continues to progress on multiple fronts supported by

3 over a decade of cumulative studies despite a recent "whipsaw" movement of controversies related

4 to the terminology and biology of "cardiac stem cells"[30,31]. Although cardiogenic potential of

5 "cardiac stem cells" remains debatable[32,33], cardioprotective effects have been repeatedly

6 demonstrated by our group and others[13,34,35,36] with "cardiac stem cells", now referred to as cCIC

7 in this report to avoid being misconstrued as cardiogenic cells. Furthermore, cardioprotective

8 effects of cCICs are enhanced by combinatorial delivery with MSCs[6]. These findings are

9 encouraging, but efficacy of such adoptive transfer cell therapies is inherently limited by multiple

10 factors including poor cell survival, engraftment, and persistence that can be overcome to some

11 extent by ex vivo cell engineering. Our group has focused upon potentiation of myocardial repair

12 through use of modified cells created by genetic engineering[9,10,14,37], fusion[8], and combinatorial

13 culture / delivery[38] (Megan Monsanto, unpublished data, [2019]). Implementation of these

14 'unnatural' approaches to create engineered cell types and combinations is deliberately intended

15 and rationally designed to overcome inherent limitations of normal mammalian myocardial that

16 lacks endogenous cellular reservoirs to repair and restore myocardial structure and function

17 following pathological damage. The rationale for CC in our initial study was to avoid issues related

18 to variable survival, engraftment, persistence, and proliferation rates of cCIC versus MSC when

19 mixing these two distinct populations together for cell therapy administration. We posited that

20 creating a novel fused hybrid CC would deliver significantly enhanced reparative activity

21 compared to each parental cell type used either alone or in mixed single cell suspensions; a

22 postulate that was validated in a syngeneic murine infarction model[8]. The next logical advance of

23 this patented technology (US Patent #20160346330A1) was to apply a comparable approach in

1   the context of human cCIC and MSC. Species-specific characteristics between murine versus

2   human biology result in differences in the creation and phenotypic properties of CC, as reinforced

3   by results in this report.

4   Comparison between human versus murine CC reveal both similarities as well as important

5   distinctions. Specifically with respect to similarities between mouse CC and hCC, there were a

6   few notable parallels including 1) variable proliferative characteristics (slow, medium, fast), 2)

7   variable CC size, 3) comparable PECAM 1 expression (intermediate level in both mouse and

8   human CCs compared to the parent cells), and 4) cardiac troponin T expression at high level

9   relative to parental lines in hCC D2 and B3 (medium and slow grower lines, respectively) similar

10   to mouse CC versus parental lines. In comparison, differences between mouse CC and hCC were

11   numerous and significant as demonstrated by 1) higher survival level compared to parental cells

12   in response to oxidative stress by hCCs, whereas murine CC survival was either similar or lower

13   than parental cells, 2) normal diploid DNA content of hCC compared to tetraploidy in murine CC,

14   3) SMA expression was lower in hCC than either parental cell, but higher in mouse CCs than the

15   cCIC parental cell, 4) cardiac troponin T expression level in hCC similar to fast growing parental

16   lines versus higher level expression in mouse CC, and 5) variable protective effects in NRCM co-

17   culture studies of hCC relative to parental cells versus similar protective effects between murine

18   CC and parental cells. Even with an admittedly small sampling size of two murine CCs and 5 hCCs

19   there are demonstrable biological and phenotypic differences between species-specific CC

20   warranting further characterization.

21   Polyploidy observed in mouse CC was notably absent from human CC lines. The diploid (2n)

22   DNA content of hCC (Figure 2) contrasts with that of murine CCs which had increased DNA

23   content[8]. Cytogenic analysis of hCC G4 further confirmed a normal karyotype with 46

21

1   chromosomes. The most straightforward interpretation of this finding is that human cell fusions

2   do not tolerate polyploidy as a permissive state for mitotic growth, unlike their murine

3   counterparts. hCCs may acquire one copy of each chromosome complement from either of the

4   parent cells leading to no change in ploidy content, despite being successfully fused. This

5   cytogenetic state eliminates concerns regarding fusion-induced increased DNA content and

6   aneuploidy which can lead to genomic instability and cellular senescence[39]. All hCCs retained

7   cellular properties corresponding to cCIC and MSCs consistent with chromosomal mosaicism in

8   somatic cells without significantly altering stem cell behavior[40].

9   MSCs mediate cell survival through secretion of pro-survival chemokines and cytokines including

10   SDF-1 and IGF-1[41,42]. hCCs expressed growth factors and cardioprotective cytokines including

11   EGF and SDF and were resistant against starvation-induced cell death (Figure 5A,C and Figure

12   6A). Similarly, hCCs demonstrated enhanced survival in response to oxidative stress (Figure 6B)

13   and attenuated necrotic cell death in response to I/R injury (Figure 6B,C). When co-cultured with

14   NRCMs, hCC G4 exhibited cardioprotective effect similar to MSCs whereas hCCs F1, D6 and D2

15   exhibited cardioprotective effect similar to cCIC with hCC D2 exhibiting the highest

16   cardioprotective activity (Figure 7). Cellular cross talk survival signals might be facilitated in CC,

17   since exosome contents such as MSC-secreted micro-RNA 21 protects c-Kit$^+$ stem cells from

18   oxidative injury through the PTEN/PI3K/Akt signaling pathway[43]. Paracrine signaling activity has

19   been suggested as the mechanistic basis for cardioprotection using cell therapy[44,45,46], so the

20   relevance of the secretome from hCCs deserves further detailed analyses to establish a putative

21   role in enhancing survival signaling. The potential contribution of cell fusion to heart regeneration

22   is essentially unexplored despite the established role of cell fusion as a reprogramming mechanism

23   leading to enhanced proliferation and growth rate in differentiated cells[47]. The findings presented

here suggest cell fusion as a reliable and stable technique to generate human hybrid cells. cCICs and MSCs are ideal cellular candidates for cell fusion. They can be consistently isolated and expanded in laboratory settings and they are well established cell candidates for cellular therapy based on the results of basic biological studies and clinical trials[4,48]. In the present study, cCICs and MSCs were used at a ratio of 2:1 but cell ratios used for fusion can influence the fate and functional potential of resultant hybrids. Therefore, modifying the cell number ratio prior to fusion could be a promising future direction leading to the design of hybrids with individualized phenotypic characteristics. Moreover, adapting cell fusion ratios for future studies may promote creation of hCCs with more consistent biological profiles.

Cell fusion is a tractable engineering approach to generate a novel cell population incorporating characteristics of two different human cardiac derived interstitial cell populations into a single cell. Hybrid CCs possess molecular and phenotypic characteristics similar to previously established murine CCs with enhanced myocardial repair potential[8]. However, cell engraftment, cardiomyogenic and reparative potential of hCCs need to be determined and are the subject of the future investigation that could support next steps toward translational application of hCCs.

Acknowledgments

1 statistical analysis of the results. All persons named in the Acknowledgments section have

2 provided the corresponding author with permission to be named in the manuscript.

3 **Source of Finding**

8 **Disclosures**

9 MA Sussman is a founding member of CardioCreate, Inc.

References

1. Li Q-H, Cao P, Vajravelu BN, Guo Y, Du J, Bolli R, Hong KU, Zhu X, Bhatnagar A, Book MJ, Nong Y, Al-Maqtari T. c-kit+ Cardiac Stem Cells Alleviate Post-Myocardial Infarction Left Ventricular Dysfunction Despite Poor Engraftment and Negligible Retention in the Recipient Heart. PLoS One. 2014;9(5):e96725.

2. Sanganalmath SK, Bolli R. Cell Therapy for Heart Failure. Circ Res. 2013;113(6):810-834.

3. Hare JM, Fishman JE, Gerstenblith G, et al. Comparison of allogeneic vs autologous bone marrow-derived mesenchymal stem cells delivered by transendocardial injection in patients with ischemic cardiomyopathy: The POSEIDON randomized trial. JAMA - J Am Med Assoc. 2012;308(22):2369-2379.

4. Slaughter MS, Chugh AR, Rokosh DG, et al. Cardiac stem cells in patients with ischaemic cardiomyopathy (SCIPIO): initial results of a randomised phase 1 trial. Lancet. 2011;378(9806):1847-1857.

5. Gerstenblith G, Johnston P V., Marbán L, Bonow RO, Marbán E, Mendizabal A, Lardo AC, Malliaras K, Wu E, Smith RR, Cingolani E, Makkar RR, Schuleri KH, Cheng K. Intracoronary Cardiosphere-Derived Cells After Myocardial Infarction. J Am Coll Cardiol. 2013;63(2):110-122.

6. Williams AR, Hatzistergos KE, Addicott B, McCall F, Carvalho D, Suncion V, Morales AR, Da Silva J, Sussman MA, Heldman AW, Hare JM. Enhanced effect of combining human cardiac stem cells and bone marrow mesenchymal stem cells to reduce infarct size and to restore cardiac function after myocardial infarction. Circulation. 2013;127(2):213-223.

7.   Mitrani RD, Traverse JH, Chugh A, et al. Rationale and Design of the CONCERT-HF Trial (Combination of Mesenchymal and c-kit + Cardiac Stem Cells As Regenerative Therapy for Heart Failure) . Circ Res. 2018;122(12):1703-1715.

8.   Quijada P, Salunga HT, Hariharan N, Cubillo JD, El-Sayed FG, Moshref M, Bala KM, Emathinger JM, De La Torre A, Ormachea L, Alvarez R, Gude NA, Sussman MA. Cardiac stem cell hybrids enhance myocardial repair. Circ Res. 2015;117(8):695-706.

9.   Fischer KM, Cottage CT, Wu W, Din S, Gude NA, Avitabile D, Quijada P, Collins BL, Fransioli J, Sussman MA. Enhancement of myocardial regeneration through genetic engineering of cardiac progenitor cells expressing pim-1 kinase. Circulation. 2009;120(21):2077-2087.

10.   Mohsin S, Khan M, Toko H, et al. Human cardiac progenitor cells engineered with Pim-I kinase enhance myocardial repair. J Am Coll Cardiol. 2012;60(14):1278-1287.

11.   Korski KI, Kubli DA, Wang BJ, Khalafalla FG, Monsanto MM, Firouzi F, Echeagaray OH, Kim T, Adamson RM, Dembitsky WP, Gustafsson ÅB, Sussman MA. Hypoxia Prevents Mitochondrial Dysfunction and Senescence in Human c-Kit+ Cardiac Progenitor Cells. Stem Cells. 2019;(9999):1-13.

12.   Monsanto MM, Dembitsky WP, Ilves K, Kim T, White KS, Mohsin S, Fisher K, Sussman MA, Broughton K, Casillas A, Wang BJ, Khalafalla FG. Concurrent Isolation of 3 Distinct Cardiac Stem Cell Populations From a Single Human Heart Biopsy. Circ Res. 2017;121(2):113-124.

13.   Gude NA, Firouzi F, Broughton KM, et al. Cardiac c-Kit Biology Revealed by Inducible Transgenesis. Circ Res. 2018;123(1):57-72.

14.   Mohsin S, Khan M, Nguyen J, Alkatib M, Siddiqi S, Hariharan N, Wallach K, Monsanto M, Gude N, Dembitsky W, Sussman MA. Rejuvenation of human cardiac progenitor cells with pim-1 kinase. Circ Res. 2013;113(10):1169-1179.

15.   Samse K, Emathinger J, Hariharan N, et al. Functional effect of Pim1 depends upon intracellular localization in human cardiac progenitor cells. J Biol Chem. 2015;290(22):13935-13947.

16.   Perlman RL. Mouse Models of Human Disease: An Evolutionary Perspective. Evol Med Public Heal. 2016;2016(1):170-176.

17.   Schoenfelder KP, Fox DT. The expanding implications of polyploidy. J Cell Biol. 2015;209(4):485-491.

18.   Coward J, Harding A. Size Does Matter: Why Polyploid Tumor Cells are Critical Drug Targets in the War on Cancer. Front Oncol. 2014;4:123-137.

19.   Avitabile D, Ormachea L, Tsai EJ, Sussman MA, Mohsin S, Monsanto M, Samse K, Joyo A, Hariharan N, Quijada P, De La Torre A, McGregor MJ. Nucleostemin Rejuvenates Cardiac Progenitor Cells and Antagonizes Myocardial Aging. J Am Coll Cardiol. 2015;65(2):133-147.

20.   Quijada P, Toko H, Fischer KM, Bailey B, Reilly P, Hunt KD, Gude NA, Avitabile D, Sussman MA. Preservation of myocardial structure is enhanced by pim-1 engineering of bone marrow cells. Circ Res. 2012;111(1):77-86.

21.   Jagsi R, Jiang J, Momoh AO, Alderman A, Giordano SH, Buchholz TA, Pierce LJ, Kronowitz SJ, Smith BD. HHS Public Access. 2017;263(2):219-227.

22.   Blackwood EA, Thuerauf DJ, Plate L, Glembotski CC, Paxman RJ, Wiseman RL, Azizi K, Kelly JW. Pharmacologic ATF6 activation confers global protection in widespread disease models by reprograming cellular proteostasis. Nat Commun. 2019;10(1):1-16.

23.   Okabayashi FM, Okada Y, Tachibanat T. A Series of Hybrid Cells Containing Different Ratios of Parental Chromosomes Formed by Two Steps of Artificial Fusion. Vol 68.; 1971. https://www.ncbi.nlm.nih.gov/pmc/articles/PMC391097/pdf/pnas00076-0045.pdf. Accessed August 8, 2019.

24.   Suetsugu A, Matsumoto T, Hasegawa K, Nakamura M, Kunisada T, Shimizu M, Saji S, Moriwaki H, Bouvet M, Hoffman RM. Color-coded Live Imaging of Heterokaryon Formation and Nuclear Fusion of Hybridizing Cancer Cells. Anticancer Res. 2016;36(8):3827-3831. http://www.ncbi.nlm.nih.gov/pubmed/27466484. Accessed August 8, 2019.

25.   Shirakata Y. Heparin-binding EGF-like growth factor accelerates keratinocyte migration and skin wound healing. J Cell Sci. 2005;118(11):2363-2370.

26.   Iwamoto R, Mekada E. ErbB and HB-EGF Signaling in Heart Development and Function. Cell Struct Funct. 2006;31(1):1-14.

27.   Yi S, Chen JR, Viallet J, Schwall RH, Nakamura T, Tsao MS. Paracrine effects of hepatocyte growth factor/scatter factor on non-small-cell lung carcinoma cell lines. Br J Cancer. 1998;77(12):2162-2170.

28.   ISLAM MR, YAMAGAMI K, YOSHII Y, YAMAUCHI N. Growth factor induced proliferation, migration, and lumen formation of rat endometrial epithelial cells in vitro. J Reprod Dev. 2016;62(3):271-278.

28

29.   Lee JG, Jung E, Heur M. Fibroblast growth factor 2 induces proliferation and fibrosis via SNAI1-mediated activation of CDK2 and ZEB1 in corneal endothelium. J Biol Chem. 2018;293(10):3758-3769.

30.   Gude NA, Sussman MA. Chasing c-Kit through the heart: Taking a broader view. Pharmacol Res. 2018;127:110-115.

31.   Khan M, Koch WJ. c-kit [+] Cardiac Stem Cells. Circ Res. 2016;118(5):783-785.

32.   Yan J, Bu L, Zhang L, et al. Resident c-kit+ cells in the heart are not cardiac stem cells. Nat Commun. 2015;6(1):8701-8710.

33.   Van Berlo JH, Kanisicak O, Maillet M, Vagnozzi RJ, Karch J, Lin SCJ, Middleton RC, Marbán E, Molkentin JD. C-kit+ cells minimally contribute cardiomyocytes to the heart. Nature. 2014;509(7500):337-341.

34.   Vajravelu BN, Hong KU, Al-Maqtari T, Cao P, Keith MCL, Wysoczynski M, Zhao J, Moore JB, Bolli R. C-Kit promotes growth and migration of human cardiac progenitor cells via the PI3KAKT and MEK-ERK Pathways. PLoS One. 2015;10(10):e0140798.

35.   Smith AJ, Torella A, Shone V, et al. Adult cardiac stem cells are multipotent and robustly myogenic: c-kit expression is necessary but not sufficient for their identification. Cell Death Differ. 2017;24(12):2101-2116.

36.   Ellison GM, Vicinanza C, Smith AJ, et al. Adult c-kitpos cardiac stem cells are necessary and sufficient for functional cardiac regeneration and repair. Cell. 2013;154(4):827-842.

37.   Sussman MA, Tuck S, Gude N, Cottage CT, Muraski J, Alvarez R, Bailey B, Avitabile D, Fischer KM, Quijada P, Collins B. Cardiac Progenitor Cell Cycling Stimulated by Pim-1

Kinase. Circ Res. 2010;106(5):891-901.

38.   Monsanto M, White K, Fisher K, Wang J SM. CardioClusters: Harnessing the Power of Multi-lineage Cardiac Stem Cells. Circ Res. 2018;121(Supp-1):A355 (Abstract).

39.   Carrera-Quintanar L, Bernad A, Samper E, Torres Y, Benguría A, Pérez RA, Ramírez JC, Roche E, Dopazo A, Enríquez JA, Torres R, Estrada JC. Human mesenchymal stem cell-replicative senescence and oxidative stress are closely linked to aneuploidy. Cell Death Dis. 2013;4(6):e691.

40.   Peterson SE, Westra JW, Rehen SK, et al. Normal human pluripotent stem cell lines exhibit pervasive mosaic aneuploidy. PLoS One. 2011;6(8):e23018.

41.   Dong F, Harvey J, Finan A, Weber K, Agarwal U, Penn MS. Myocardial CXCR4 expression is required for mesenchymal stem cell mediated repair following acute myocardial infarction. Circulation. 2012;126(3):314-324.

42.   Herrmann JL, Wang Y, Meldrum DR, Abarbanell AM, Poynter JA, Manukyan MC, Weil BR, Brewster BD. Intracoronary Mesenchymal Stem Cells Promote Postischemic Myocardial Functional Recovery, Decrease Inflammation, and Reduce Apoptosis via a Signal Transducer and Activator of Transcription 3 Mechanism. J Am Coll Surg. 2011;213(2):253-260.

43.   Shi B, Wang Y, Zhao R, Long X, Deng W, Wang Z. Bone marrow mesenchymal stem cell-derived exosomal miR-21 protects C-kit+ cardiac stem cells from oxidative injury through the PTEN/PI3K/Akt axis. PLoS One. 2018;13(2):e0191616.

44.   Angelos MG, Noor M, Dougherty JA, Kumar N, Khan M, Chen C-A, Khan M. Extracellular

Vesicles Released by Human Induced-Pluripotent Stem Cell-Derived Cardiomyocytes Promote Angiogenesis. Front Physiol. 2018;9:1794-1807.

45.   Moore JB, Tang XL, Zhao J, Fischer AG, Wu WJ, Uchida S, Gumpert AM, Stowers H, Wysoczynski M, Bolli R. Epigenetically modified cardiac mesenchymal stromal cells limit myocardial fibrosis and promote functional recovery in a model of chronic ischemic cardiomyopathy. Basic Res Cardiol. 2018;114(1):3-26.

46.   Balbi C, Bollini S. Fetal and perinatal stem cells in cardiac regeneration: Moving forward to the paracrine era. Placenta. 2017;59:96-106.

47.   Cowan CA, Atienza J, Melton DA, Eggan K. Developmental Biology: Nuclear reprogramming of somatic cells after fusion with human embryonic stem cells. Science (80-). 2005;309(5739):1369-1373.

48.   Davani S. Mesenchymal Progenitor Cells Differentiate into an Endothelial Phenotype, Enhance Vascular Density, and Improve Heart Function in a Rat Cellular Cardiomyoplasty Model. Circulation. 2003;108(90101):253II--258.

Table 1. List of fusions

| Fusions	% Yield	hCC analyzed
1	% 4	G4
2	% 3.1	D6
3	% 1.5	F1
4	% 1.3	B3
5	% 1.2	D2
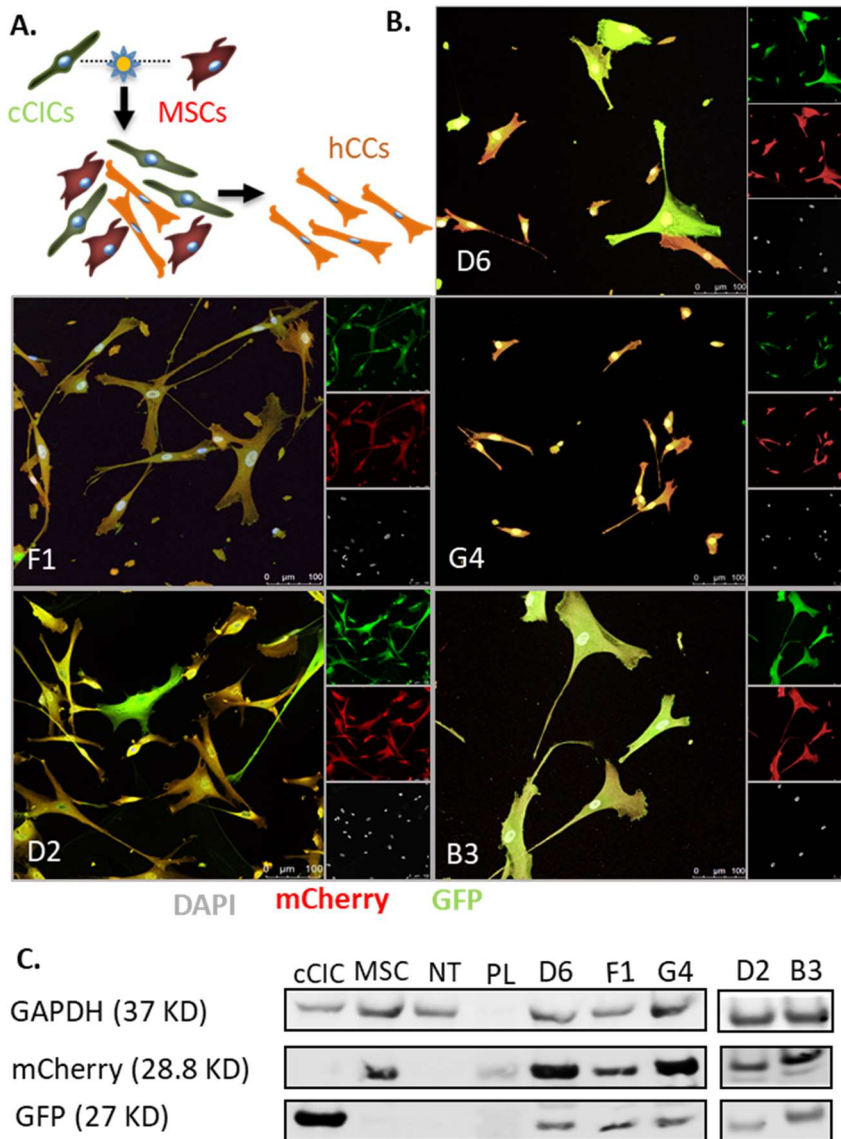
Figure 1. hCCs are created from cCIC and MSC cell fusion. A. Schematic of the cell fusion. Phase A: fusion-suspension of cCICs and MSCs. Phase B: initial fused cells undergo mitotic event to combine chromatin content. Phase C: Sorting of successfully fused cell. **B.** ICC of the hCCs for GFP and mCherry. **C.** Immunoblot analysis of cCIC-GFP, MSC-mCherry, Non-Transduced (NT) MSC, and hCCs. PL: protein ladder. GAPDH is used as the loading control.
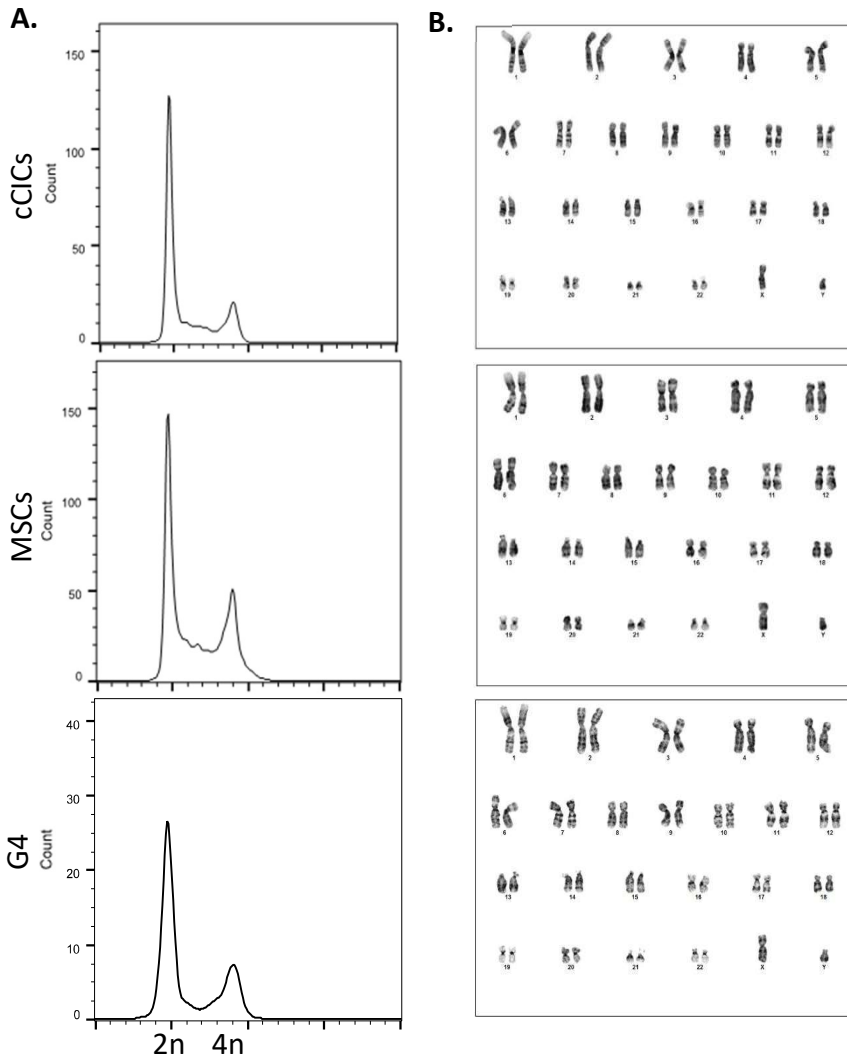
Figure 2. hCCs reveal ploidy status and DNA content corresponding to the parent cells. A.

Flow Cytometry plots for PI/RNAse staining of parent cells and hCCs, G4. N=3 independent

experiments. **B.** Cytogenetic analysis of parent cells and hCC, G4.
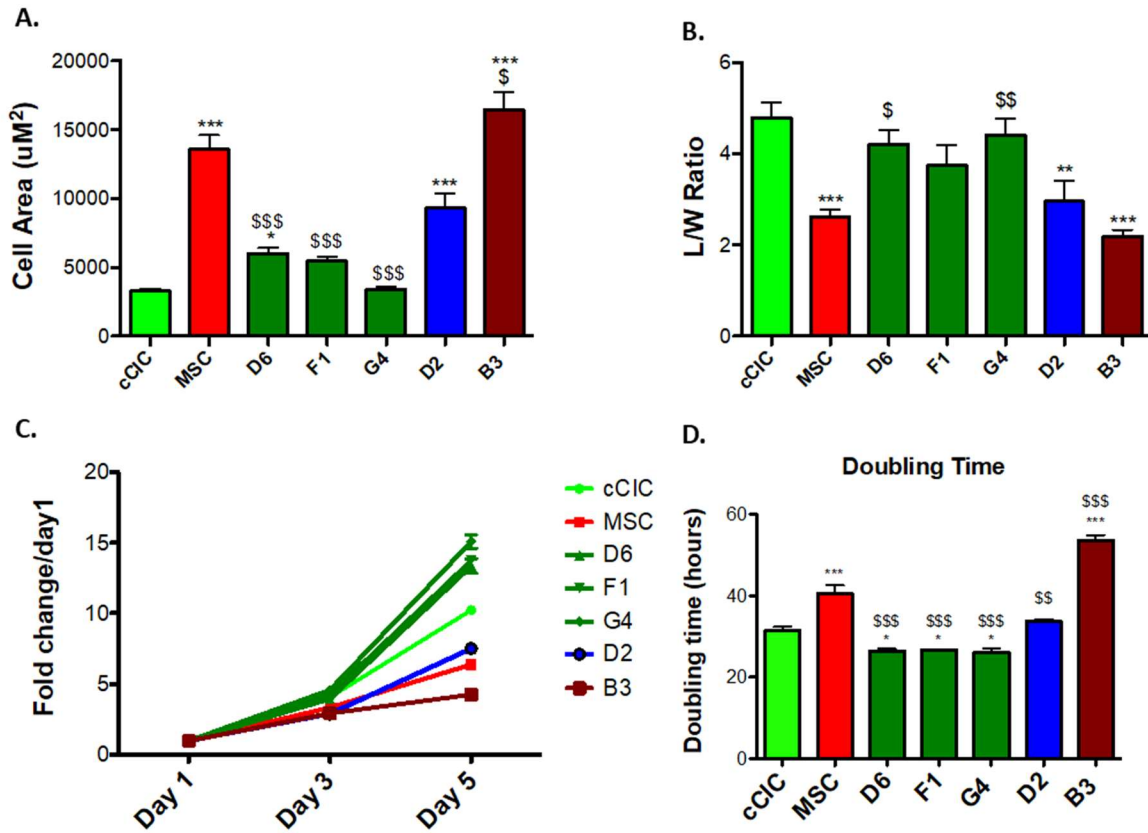
Figure 3. Morphometric and proliferative characteristics of hCCs. **A.** Cell surface area and **B.** length to width ratio of the parent cells and hCCs. **C.** Proliferation rate of parent cells and hCCs represented as fold change over day 1, and **D.** cell doubling time represented in hours. N=3 independent experiments. Statistical analysis was performed by One-Way ANOVA multiple comparison with Dunnett. *$P<0.05$ Vs cCIC, **$P<0.001$ Vs cCIC, ***$P< 0.0001$ Vs cCIC, $$P<0.05$ Vs MSC, $$$P<0.001$ Vs MSC, $$$$P<0.0001$ Vs MSC. Error bars are ± SEM.
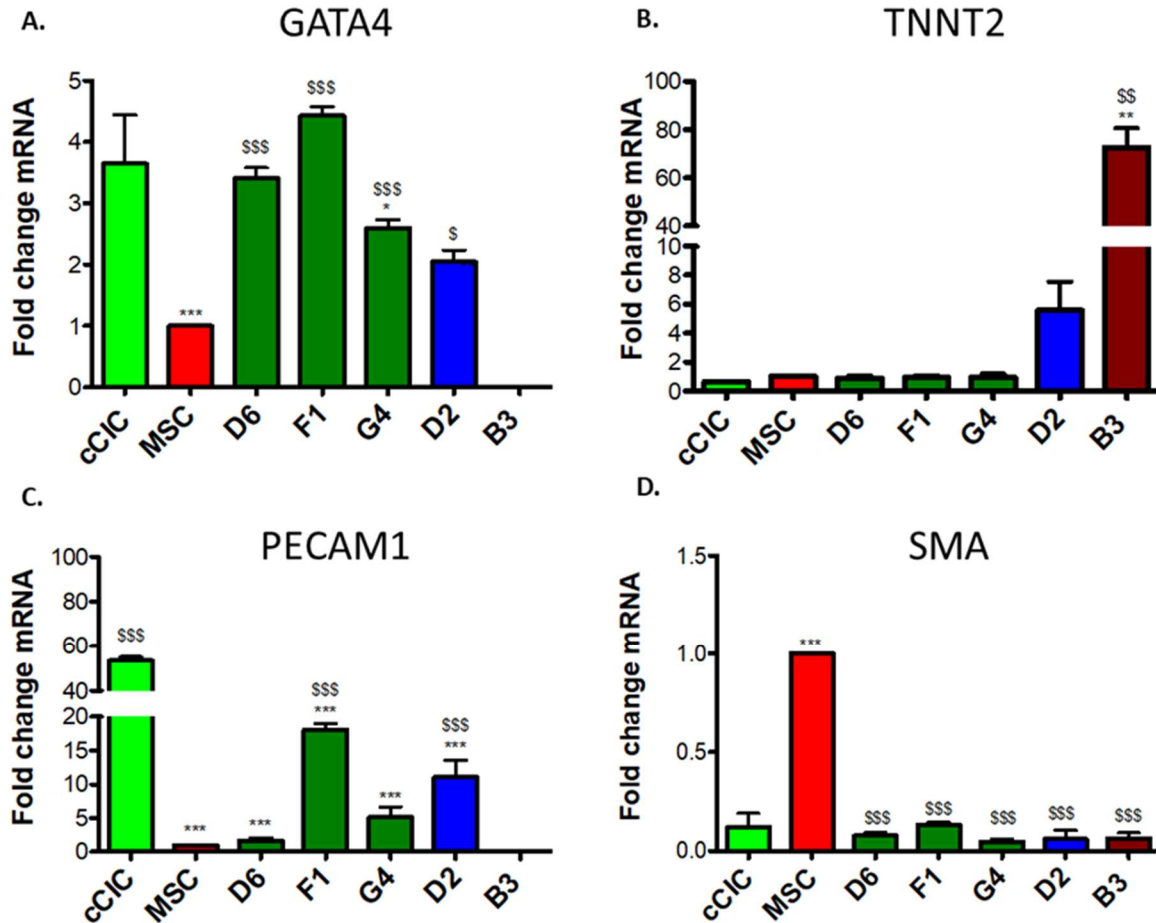
Figure 4. hCCs exhibit variable expression level of cardiomyogenic commitment markers. mRNA expression level of **A.** GATA4, **B.** TNNT2, **C.** PECAM1, and **D.** SMA for parent cells and hCCs. N=3 independent experiments, 3 replicates per group per experiment. All genes expression is normalized to ribosomal 18s and represented as a fold change relative to MSCs. Statistical analysis was performed by One-Way ANOVA multiple comparison with Dunnett. *P<0.05 Vs cCIC, **P<0.001 Vs cCIC, ***P< 0.0001 Vs cCIC, $P<0.05 Vs MSC, $$P<0.001 Vs MSC, $$$P<0.0001 Vs MSC. Error bars are ± SEM.

36
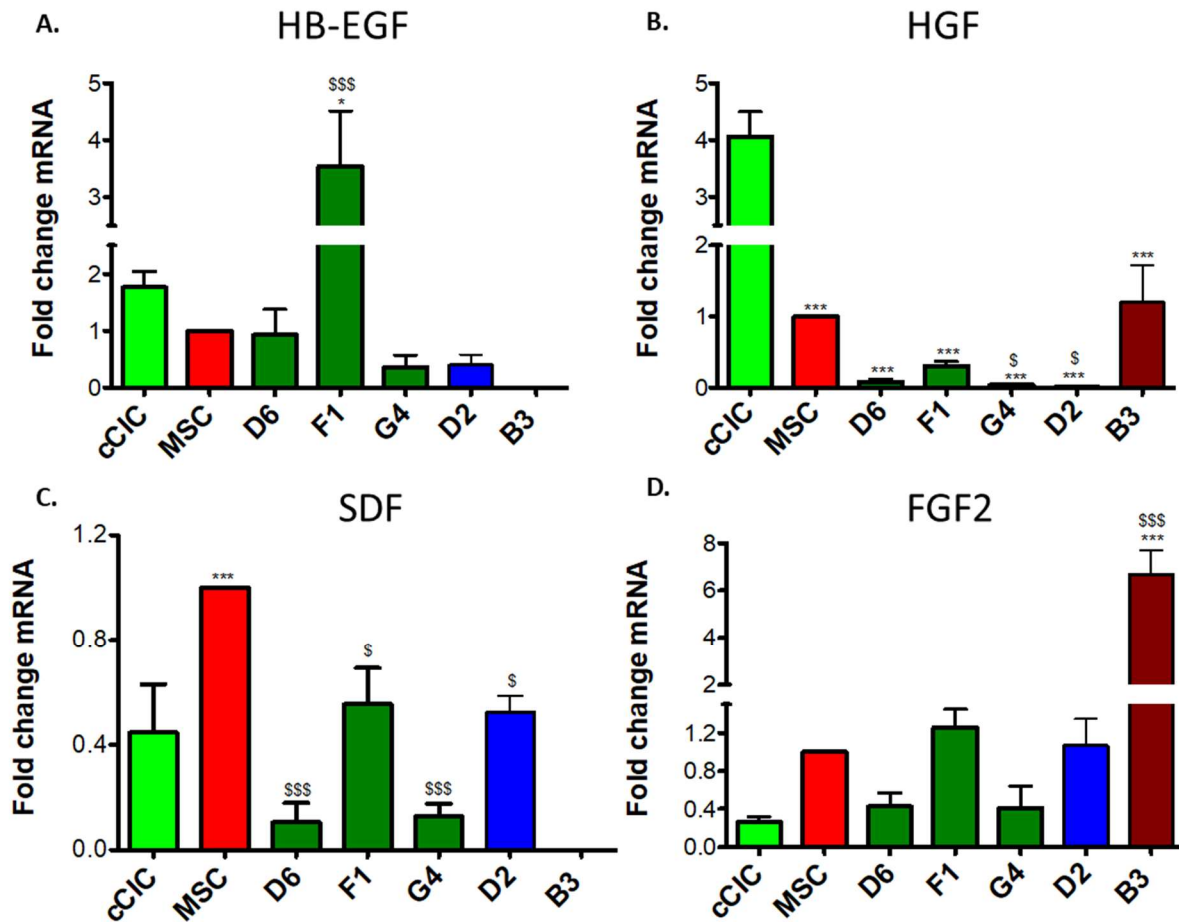
Figure 5. hCCs exhibit variable secretory gene profiles. mRNA expression level of **A.** HB-EGF, **B.** HGF, **C.** SDF, and **D.** FGF2. N=3 independent experiments, 3 replicates per group per experiment. All genes expression is normalized to ribosomal 18s and represented as a fold change relative to MSCs. Statistical analysis was performed by One-Way ANOVA multiple comparison with Dunnett. *P<0.05 Vs cCIC, **P<0.001 Vs cCIC, ***P< 0.0001 Vs cCIC, $P<0.05 Vs MSC, $$P<0.001 Vs MSC, $$$P<0.0001 Vs MSC. Error bars are ± SEM.
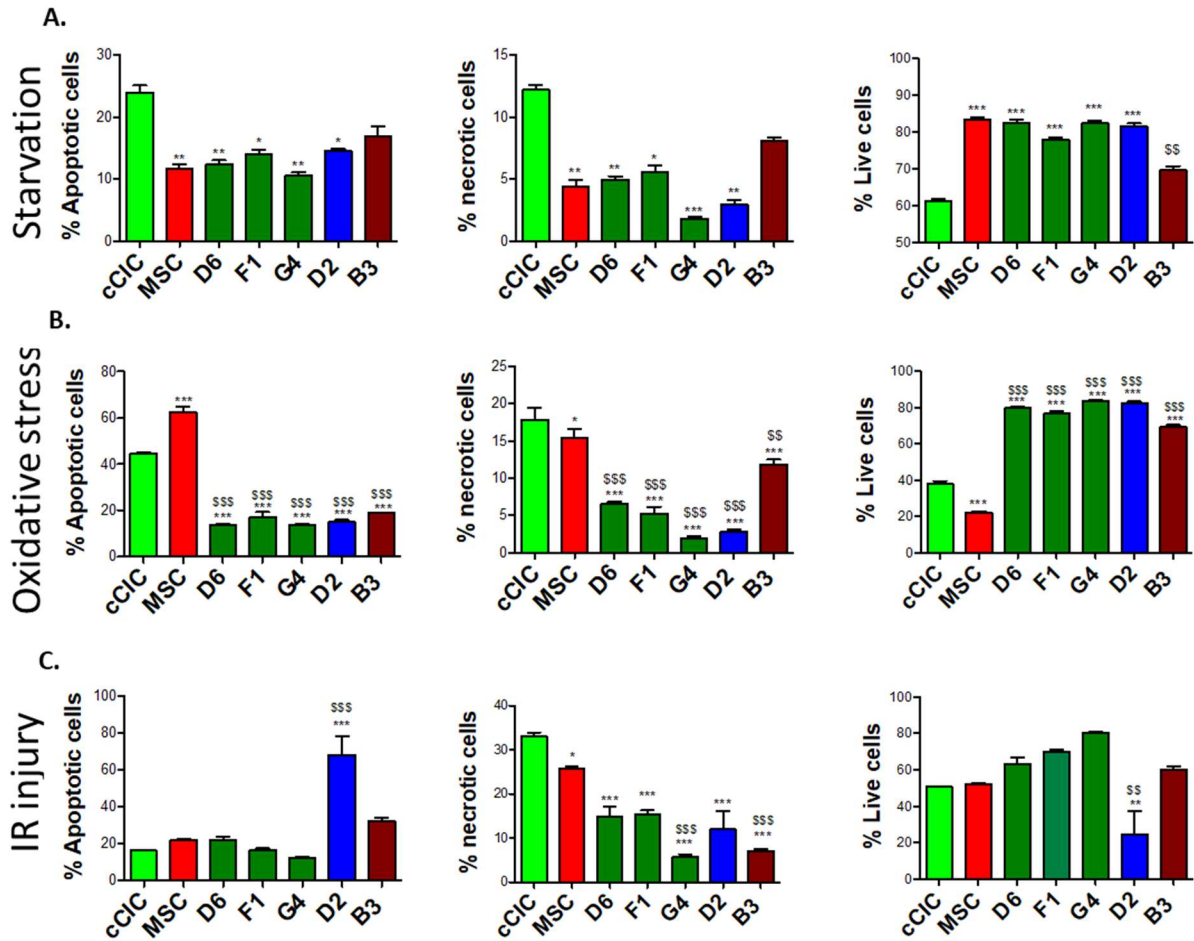
Figure 6. hCCs demonstrate enhanced survival in response to stress. Percentage of apoptotic, necrotic and live cells following **A.** serum starvation, **B.** oxidative stress, and **C.** IR injury. N=3 independent experiments. Statistical analysis was performed by Two-Way ANOVA multiple comparison with Tukey. *P<0.05 Vs cCIC, **P<0.001 Vs cCIC, ***P< 0.0001 Vs cCIC, $P<0.05 Vs MSC, $$P<0.001 Vs MSC, $$$P<0.0001 Vs MSC. Error bars are ± SEM.
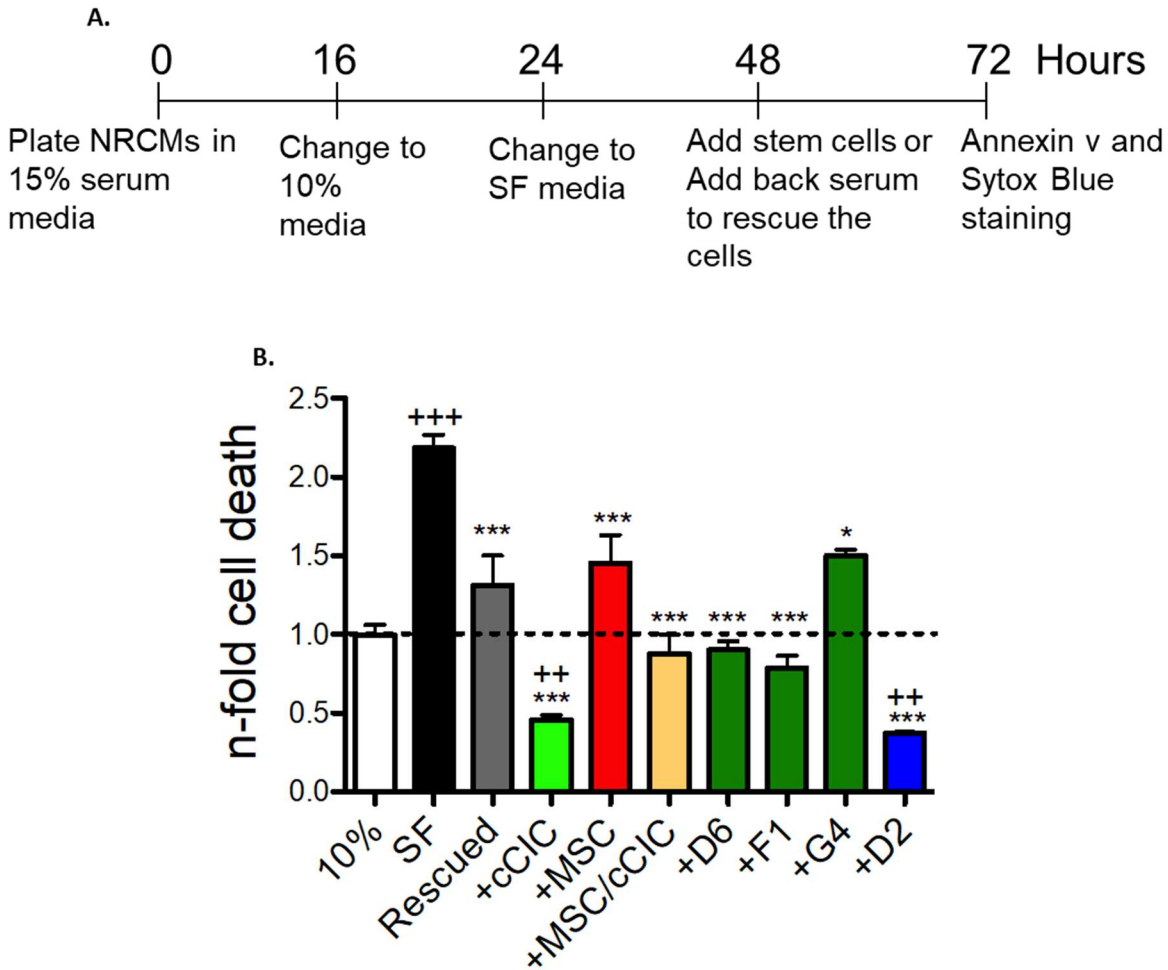
Figure 7. hCCs promote cardiomyocytes survival in response to serum deprivation. A. NRCM co-culture protocol. **B.** Cardiomyocytes cell death in 10% serum media (10%), serum free media (SF), rescued and in presence of cCICs, MSCs, combinatorial group of MSCs and cCICs (+MSCs/cCICs), D6, F1, G4 and D2. Values presented are fold change of Annexin v$^+$ Sytox Blue$^+$ cells relative to 10% serum media (also represented as dashed line, 1.0). N=3 independent experiments. Statistical analysis was performed by One-Way ANOVA multiple comparison with Dunnett. *P<0.05 Vs SF, ***P< 0.001 Vs SF, ++ P<0.01 Vs 10%, +++ P<0.001 Vs 10%.